Geosciences Journal
Vol. 17, No. 2, p. 163 − 172, June 2013
DOI 10.1007/s12303-013-0010-6

Possible origin of coastal sands and their long-term distribution along the high slope-gradient, wave-dominated eastern coast, Korea

Sang Hoon Lee*
Hee Jun Lee
Jun-Yong Park
Eui Young Jeong
Jeseon Yoon
Korea Institute of Ocean Science and Technology, Ansan, 425-600, Republic of Korea

Ho Kyung Ha
Korea Polar Research Institute, Incheon 406-840, Republic of Korea

Chang Woong Shin
Chanhong Park
Korea Institute of Ocean Science and Technology, Ansan, 425-600, Republic of Korea

ABSTRACT: This study aims to investigate possible source and long-term distributional patterns of coastal sands in the high slope-gradient, wave-dominated coast with no large rivers, eastern Korea. Chirp (2–7 kHz) seismic profiles show that the coastal sand deposits, the uppermost transparent layer, are up to 7.1 m thick off small, mountainous stream mouths, and thins laterally, showing a radial distribution from the stream mouths with a slightly SE-skewed elongated (i.e., alongshore) geometry. These features suggest that the terrigenous coarse sediments emptied by the streams during the summer flash flooding season have been a major source to the adjacent coastal sands. Hydrodynamic measurements with benthic tripod systems indicate that alongshore currents occurring during episodic storms play a significant role in the displacement of the coastal sands toward the southeast, resulting in the slightly SE-skewed elongated (i.e., alongshore) distributional geometry of the sands.

Key words: coastal sands, source, distribution, sediment transport, East Sea

1. INTRODUCTION

Coastal sands have been extensively paid attention because these sands are directly linked with economic and environmental concerns such as beach erosion, benthic habitat, etc. Natural environmental changes, such as sea-level rise and the increase in intensity and frequency of storms, and the increasing human activities or development in coastal areas have exacerbated the unsteadiness of coastal sands. Many studies using sophisticated hydrodynamic instruments have extensively unraveled various physical or hydrodynamic processes on coastal sand transport (Dyer, 1986; Fredsøe and Deigaard, 1992; Van Rijn, 1993; Komar, 1998; Soulsby, 1997). Modeling studies with some dispersed hydrodynamic data have recently tried to predict short-term changes in transport (or distribution) patterns of coastal sands (Soomere et al., 2008; Roelvink et al., 2009; McCall et al., 2010). Exact prediction of mid- to long-term changes in patterns of transport and distribution of coastal sands, however, necessarily needs regional-scale geological observations on the spatial and temporal variations of the coastal sands in terms of source-to-sink (Snedden and Nummedal, 1991; Sexton et al., 1992; Giosan et al., 2005). The source-to-sink information on coastal sands would, therefore, be crucial in understanding the responses of coastal sands to the natural and artificial environmental changes.

The eastern coast of Korea is characterized by the relatively straight coastline, the absence of large rivers and the high slope gradient associated with the mountainous hinterlands (Taeback Mountains). As a result, the eastern coast is dominated by waves with a microtidal regime, forming beaches and coastal offshore sands under the absence of large rivers. During the past three decades, massive coastal developments along the eastern coast of Korea have been significantly altering the topo-bathymetric pattern of the coastal zones, resulting in serious problems of coastal erosion. In order to resolve the problems of coastal erosion along the eastern coast of Korea, the geological and hydrodynamic studies for understanding the transport processes and budget of coastal sands have been commenced from 2008.

The study area is a coastal region about 9 km long and up to 60 m deep, encompassing beaches, small streams, and the sandy coastal offshore which often involves rocky seabeds in patch, a typical geomorphological assortment in the eastern coast of Korea (Fig. 1). This paper documents the possible sources of the coastal sands and their long-term distribution using high-resolution shallow seismic, bathymetric, and seafloor back-scattering data with supplementary hydrodynamic data collected from benthic tripod systems. This study provides important clues to understand the origins and distributional patterns of the coastal sands along the eastern coast of Korea.

*Corresponding author: sanglee@kordi.re.kr

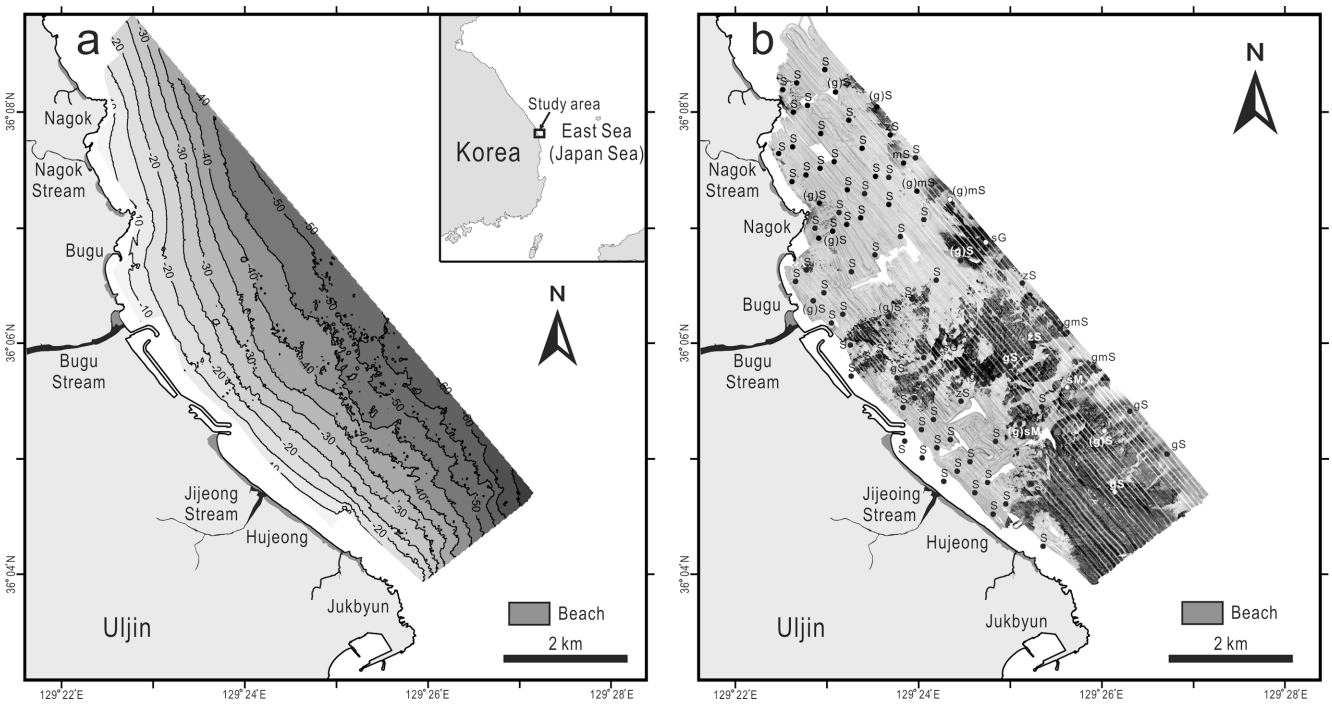

Fig. 1. (a) Bathymetry of the study area. Inset map indicates the study area. Contour interval is 5 m. (b) Back-scattering images of the seabed in the study area. Weak (white) back-scattering areas represent sandy sediments and strong (black) back-scattering areas indicate exposed rock basements. Dots with letters denote types of surface sediments. sG = sandy gravel; S = sand; gS = gravelly sand; gmS = gravelly muddy sand; zS = silty sand.

2. GEOLOGICAL AND OCEANOGRAPHICAL SETTING

The study area is characterized by relatively straight coastline which is occasionally punctuated by promontories of rocky headlands (Nagok, Bugu and Jukbyun) and artificial facilities associated with nuclear power plants (Fig. 1). Beaches are generally present between the rocky headlands. Especially, the Hujeong beach, about 3.4 km long, is well developed between the Bugu and Jukbyun headlands. The seabed is sloping to the NE, i.e., perpendicular to the shoreline, and less than 1.65° in slope gradient. It is relatively smooth, but often interrupted by exposed rocky basements (Fig. 1). In the study area, annual precipitation over the past decade ranges from 809.1 to 1789.7 mm (KMA, 2009). The precipitation is heavily concentrated in the summer flash

Fig. 2. A photo showing the mouth opening of Jijeong Stream for a short period of the summer flash flooding. In 9 and 12 July 2009, the daily precipitation was 51 and 53.5 mm, respectively. By this flash flooding, the mouth of Jijeong Stream opened to the sea with 13.5 m in width and 2.7 m in depth. A person in the circle indicates the scale.

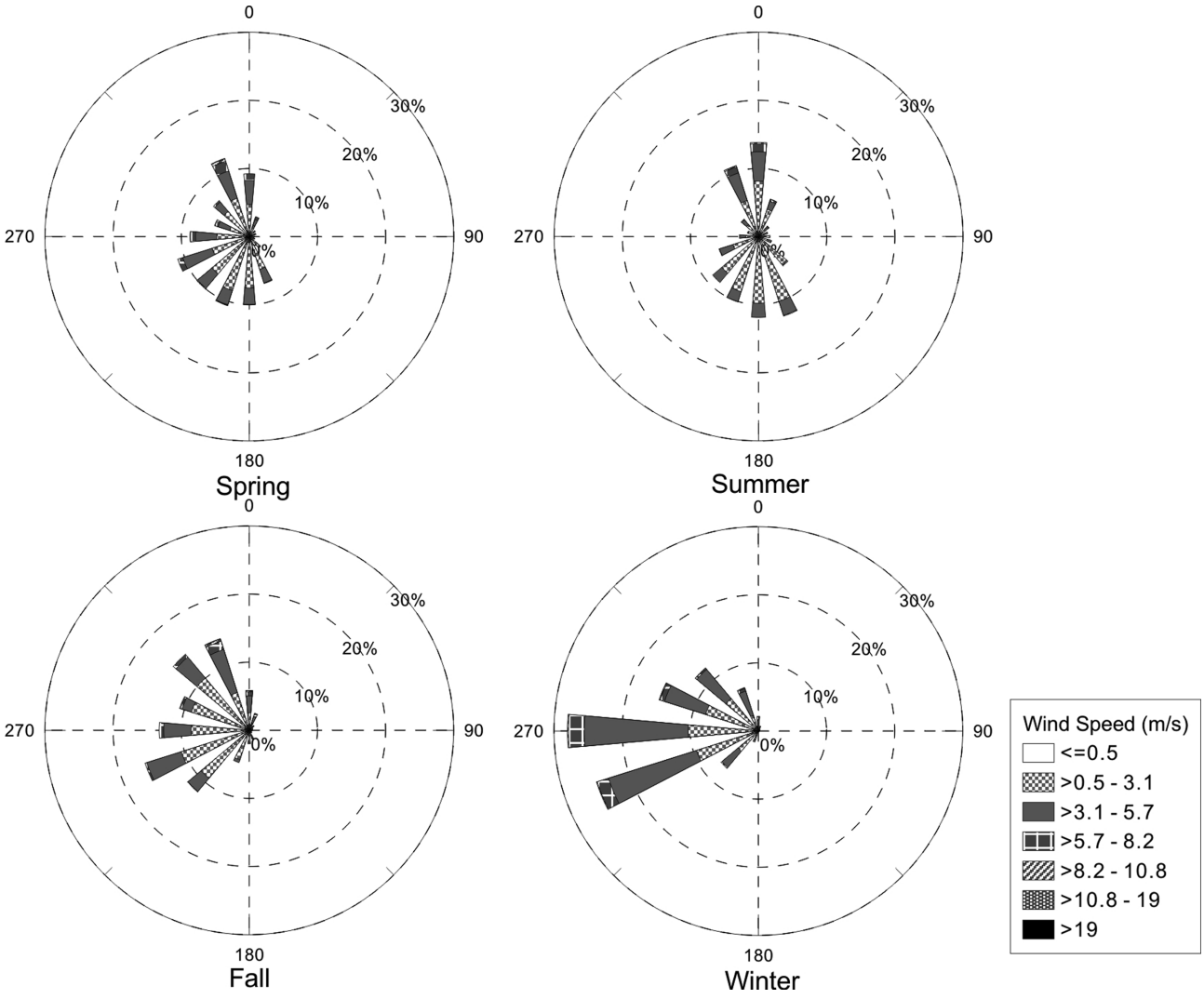

Fig. 3. Seasonal wind rose (1978–2007) of daily mean wind speed and direction at Uljin weather station (36°59'N, 124°24'E) close to the study area. Durations of spring, summer, fall, and winter seasons are March–May, June–August, September–November, and December–February, respectively. After KMA (2009).

flooding season (June-September) during which the integrated rainfall measures 491.4–1111.8 mm (mean, 831.1 mm) accounting for 57.2–76.5% of the annual precipitation. In the study area, three streams (Nagok, Bugu, and Jijeong) flow to the sea. Total drainage area of these streams is about 86.3 km^2 with steep slope gradients of 2.23–6.28°. The Bugu stream shows slope gradient of 1.43°. The Jijeong stream, the smallest one, is generally blocked by the beach except for a short period of summer flash flooding. On 9th and 12th of July 2009, the daily precipitation was 51 and 53.5 mm, respectively. By this flash flooding, the mouth of Jijeong Stream opened to the sea with 13.5 m in width and 2.7 m in depth (Fig. 2).

The 30-year (1978–2007) observations of winds from a weather station near the study area indicate that the wintertime winds between December and February are strongest, blowing mostly from the west with maximum speeds over 5 m/s (KMA, 2009; Fig. 3). In general, the occurrence of the northeasterly and southeasterly winds is virtually meager throughout the year. The waves at a location 8.5 km offshore from the study area were hindcasted from the 2008 wind data using WAVEWATCH III model (NIMR, 2009; Fig. 4). Most of the waves were estimated to propagate SW or S regardless of seasons. In particular, the winter waves were collectively in this direction with the highest frequencies of wave heights of 1–2 m. The study area is microtidal with averages of 0.16 and 0.09 m for spring and neap tidal ranges, respectively (Lee, 1999). Accordingly, tidal currents are weak and flood and ebb currents flow SE and NW, respectively.

3. MATERIALS AND METHODS

In 2008–2009, bathymetric and backscattering data were collected in the offshore area using a high-frequency (300

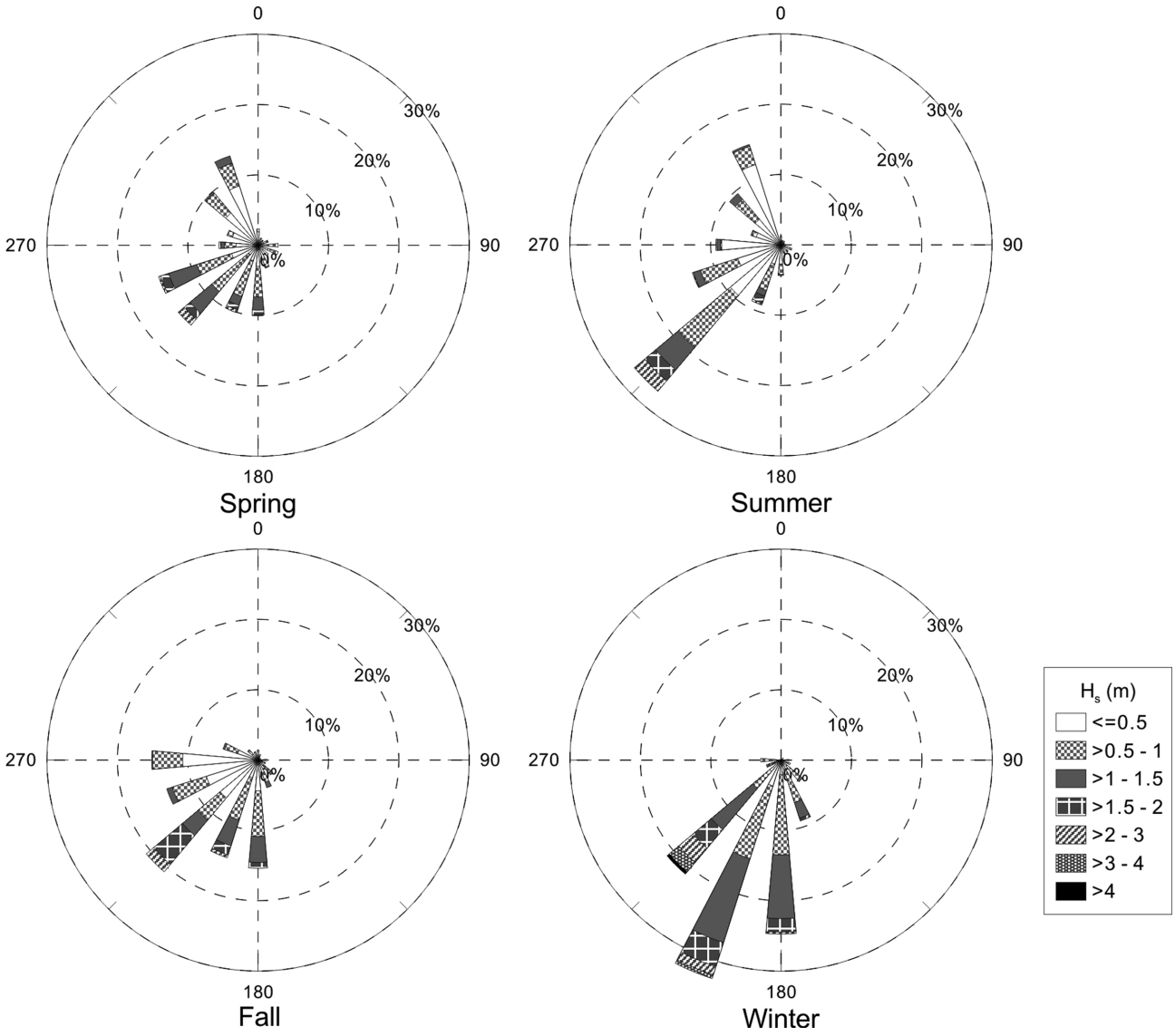

Fig. 4. Seasonal wave rose evaluated from the 2008 wind data. Durations of the seasons are the same as in Figure 3. Hs = significant wave height. After NIMR (2009).

kHz) multi-beam echo sounder (Kongsberg, EM-3002). The tracklines were mostly aligned NW–SE, parallel to the shoreline, with spacing intervals of 10–50 m. For the calibration of bathymetric data, sonic speeds were measured three times a day using a sound velocity and pressure smart sensor (Applied Microsystems, Minos SVP). High-resolution seabed images were obtained from the acoustic back-scattering data. About 97 line-km of high-resolution subbottom profiles were acquired using a Chirp (2–7 kHz) profiling system (Datasonics, CAP-6000) (Fig. 5). Navigation was controlled using a DGPS (Trimble, 4000RS/DS) with an accuracy of <5 m.

In order to reveal textural characteristics of the seabed and to compare them with the back-scattering characters, 86 surface sediments were collected using a grab sampler (Fig. 1b). Grain size analysis was conducted using standard sieves at 0.5–ϕ intervals and a Micrometric Sedigraph 5100 for sand (>63 μm) and mud (<63 μm) fractions, respectively. Sediment classification follows the scheme of Folk (1954).

The benthic tripods, called TISDOS, were deployed at two stations JB-4 (nearshore, 5 m deep) and JB-6 (offshore, 19 m deep) in September 2008 (Fig. 5). A downward-looking 1.2-MHz acoustic Doppler current profiler (ADCP, RDI) measured profiles of flow velocity and acoustic backscattering strength for the lowest 1.5 m of water column with 0.1-m bin intervals. The pulse-to-pulse coherent mode (mode-11) was selected to acquire the high spatial and temporal resolutions. A downward-looking 5-MHz acoustic Doppler velocimeter (ADV, SonTek) was mounted at 0.48 m above bed (mab) with a sampling rate of 8 Hz. The sampling vol-

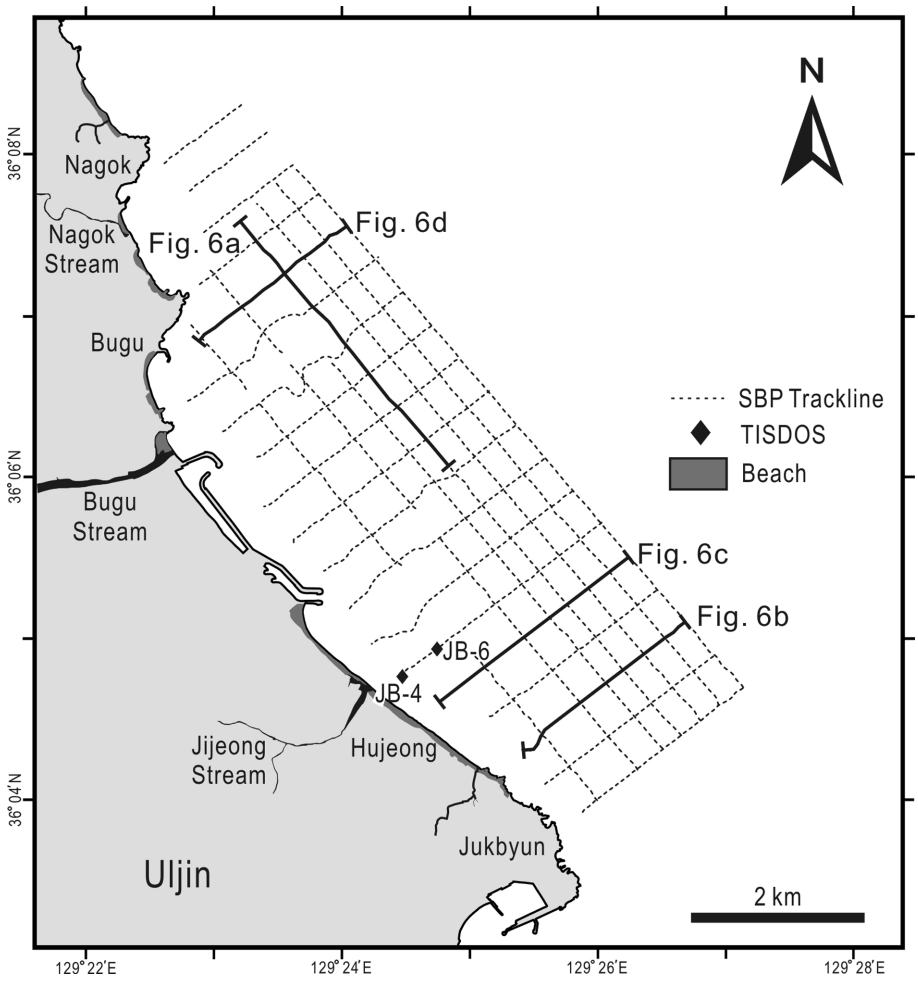

Fig. 5. Tracklines of Chirp (2–7 kHz) profiling (dotted lines) and location of grab samples (dots) and TISDOS (diamonds). Bold lines indicate the location of Figures 6a–d.

ume was located at 0.3 mab due to blanking distance. Two synchronized optical back-scattering sensors (OBS) were installed at 0.3 and 1.0 mab to measure suspended sediment concentrations (SSC). The changes in water surface elevation were measured with a pressure sensor (Digiquartz) at 2 Hz, and were used to evaluate water depth with corrections for effects of depth attenuation through linear wave theory. Wave statistics such as the significant wave height (H_s) and the peak wave period (T_p) were calculated by spectral analysis approach to the oscillatory part of the demeaned water-surface elevation records (Longuet-Higgins, 1952).

4. RESULTS

In high-resolution back-scattering image, the seabed showing weak (white) intensity consists mostly of sands (>90% sand content) (Fig. 1b). In Chirp (2–7 kHz) profiles, this sandy seabed is characterized by the uppermost transparent layer overlying the slightly irregular prolonged subbottom echoes (Fig. 6). These prolonged subbottom echoes are nearly flat in NW–SE (i.e., alongshore) direction and offshore inclined in NE–SW (i.e., cross-shore) direction, respectively (Fig. 6). The transparent acoustic character in high-frequency (2–10 kHz) subbottom profiles can be ascribed to homogenous sediments (Damuth, 1980), suggesting that the subsurface sediments also consist of sandy materials. These coastal sand deposits are relatively thick (up to 7.1 m) in front of each stream mouth (Fig. 7), and are thinning in both offshore and alongshore directions forming the wedge geometry in cross section (Fig. 6). In plan view of isopach map, the coastal sand deposits show a radial distribution from the stream mouths with a slightly SE-skewed (i.e., shoreline-parallel) elongated geometry (Fig. 7).

In back-scattering image, the seafloor showing strong (black) intensity represents rock basements which are dominant in the middle and southeastern parts of the study area (Fig. 1b). The rock basements are characterized by rugged, strong bottom echoes and prolonged subsurface echoes in Chirp profiles (Fig. 6). On the topographic lows in the rock basements, the gravelly/muddy sands or sandy gravels are often present as thin (<0.1 m) veneers (Figs. 1b and 6).

The sands off the stream mouths have mean size of about 3.0ϕ (Fig. 8). Mean size of the coastal sands then increases to 2.6ϕ offshore (5–30 m deep) and to 1.6ϕ in nearshore (<5

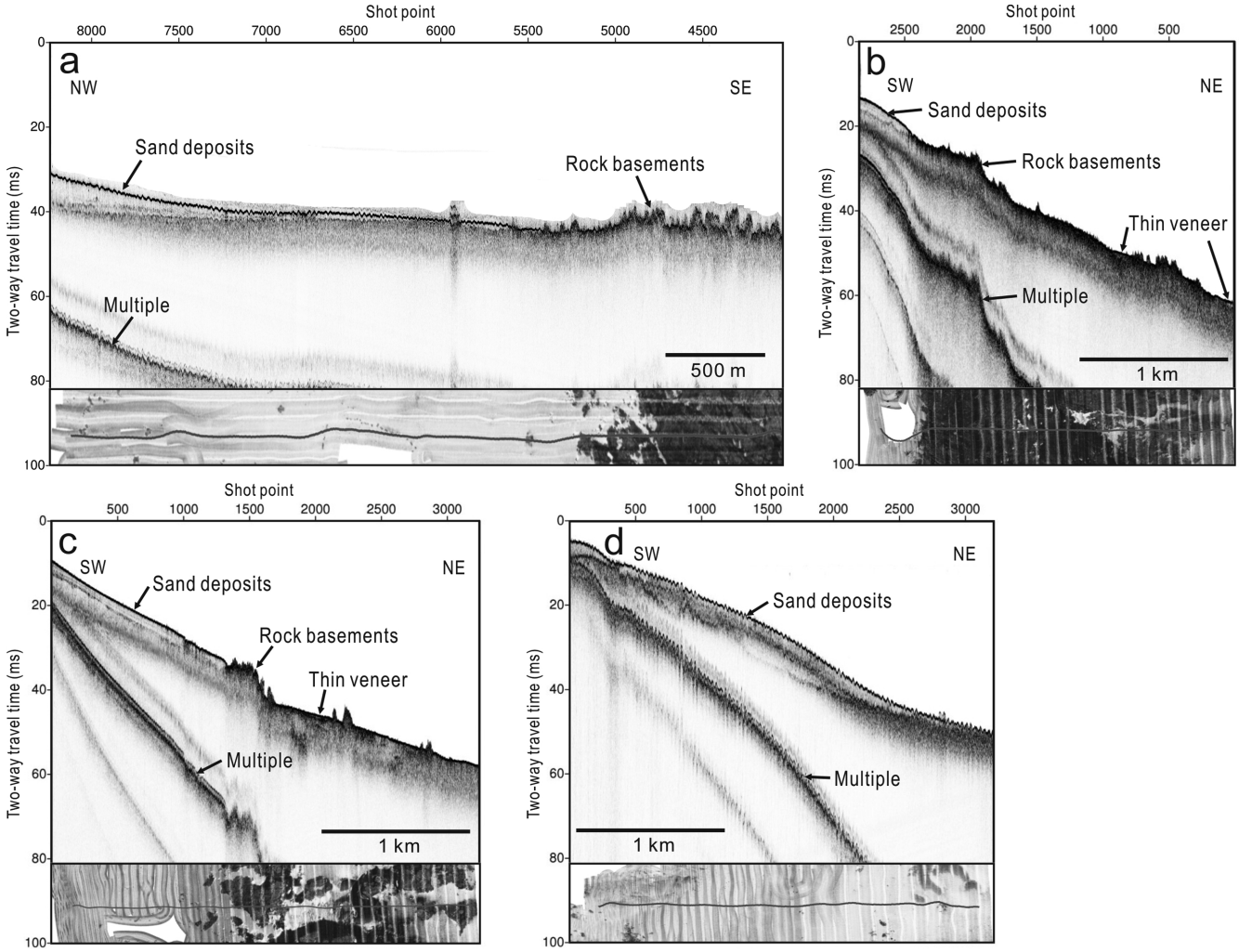

Fig. 6. Representative Chirp (2–7 kHz) profiles. For location of each profile, see Figure 5. Note the laterally wedged, acoustically transparent coastal sand deposits upon the slightly irregular prolonged layers. In (a)–(d), the lower part shows the back-scattering image of the seabed along the trackline of each profile (bold line).

m deep) (Fig. 8). Furthermore, the standard deviation (i.e., sorting) of coastal sands decreases from 1.0–1.2ϕ offshore to less than 0.8ϕ in nearshore, i.e., the sands become increasingly sorted onshore.

The TISDOS time-series data from stations JB-4 and JB-6 obtained during the period of September 26–29 (269–272 days), 2008 were chosen to describe in detail hydrodynamic characteristics and relevant sediment transport in the bottom boundary layer (Fig. 9). The seabed of the two stations was composed purely of sands with mean size increasing onshore 0.177 mm or 2.5ϕ (station JB-6) to 0.403 mm or 1.3ϕ (station JB-4). A storm accompanied by northerly winds with speeds exceeding 15 m/s passed amid 269 days (Fig. 9a). During the storm, the wave height ranged between 0.8 and 1.2 m with a maximum of 1.9 m and the wave period between 6 and 7 s except for the highest waves of which the period reaches 8.6 s (Figs. 9b and f). The ratio of the wave height to water depth was consistently evaluated at <0.35 even for the shallower station JB-4. The strong winds during the storm peak generated conspicuous mean currents with the cross-shore and alongshore components directing offshore and to the SE, respectively (Figs. 9c and d); the speeds of the two components reached up to 0.06 and 0.17 m/s, respectively. Over the remaining period of the storm, however, the mean currents were meager.

At JB-4 site (5 m water depth), the maximum wave height or orbital velocity (0.8 m/s) was lagged about 8 hours behind the maximum wind speed of 16 m/s (Figs. 9a, b, and e). Once the orbital velocity at this site was higher than about 0.2 m/s (corresponding approximately to 0.5 m of the wave height) on 269.2 days, the bottom sediments rapidly undertook erosion and resuspension (Fig. 9h). This suggests that the value of 0.2 m/s is a critical velocity for suspension threshold for the bottom sands in the nearshore of the study area. While resuspension at JB-4 site was maintained during the entire period of storm, the ejection level of sediment

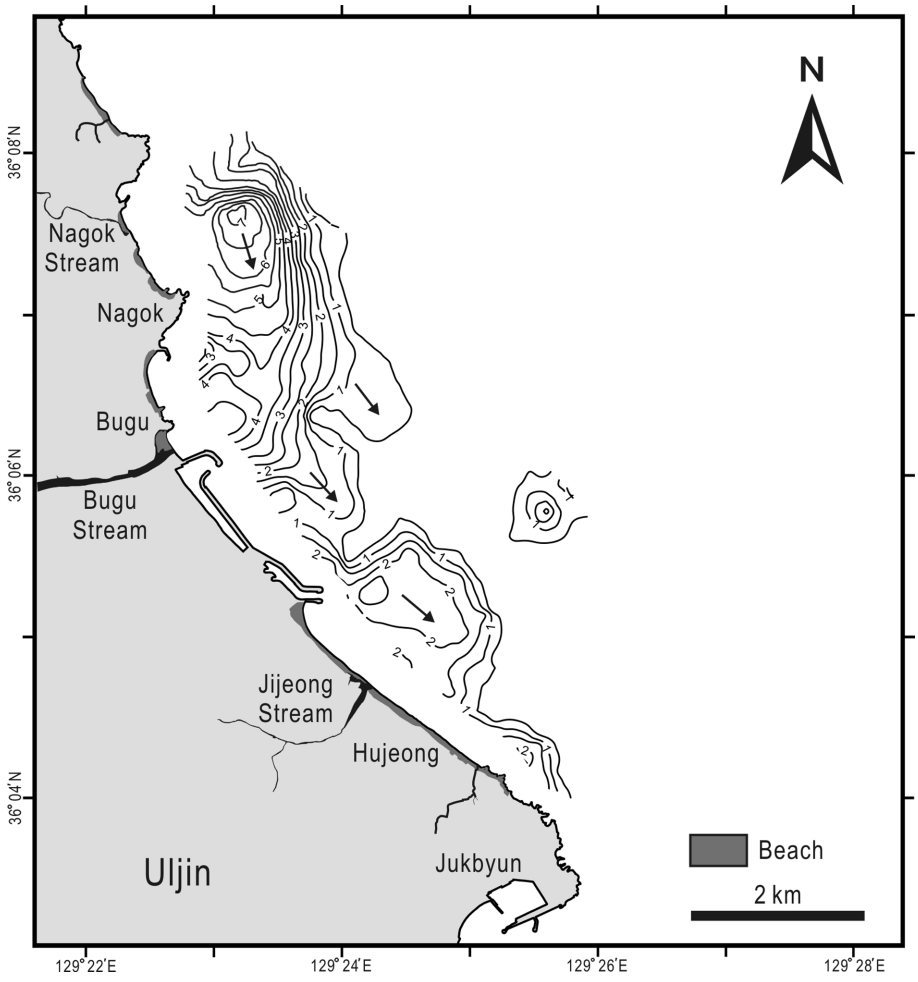

Fig. 7. Isopach map of the coastal sand deposits based on estimated thicknesses of the uppermost transparent layer in Chirp (2–7 kHz) profiles. Note that the deposits are thickest off the stream mouths. Arrows indicate a slightly SE-skewed (i.e., alongshore) elongated distributional geometry of the coastal sand deposits.

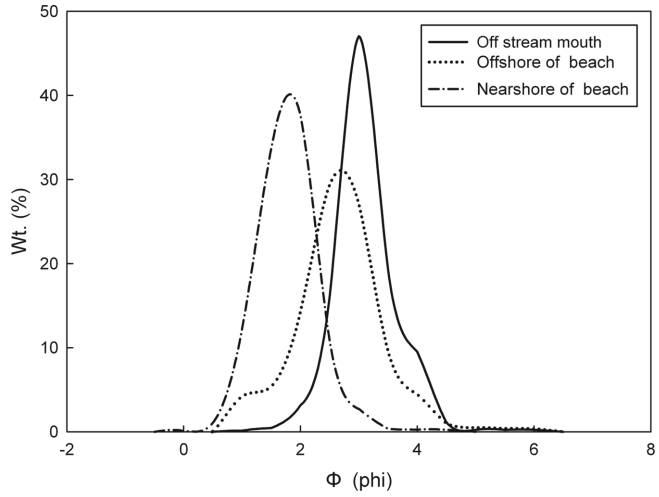

Fig. 8. Average frequency curves of grain size for sands off stream mouths, offshore and nearshore of the beach. The three provinces involve sampling sites around the stream mouths of Nagok and Bugu, 5–30 m deep, and <5 m deep, respectively. Each curve stands for an average of 5 samples representative of the corresponding province. Note that mean size is finest (3.0ϕ) off the stream mouths and then increases to 2.6ϕ offshore to 1.6ϕ in the nearshore.

reached up to approximately 1 mab at the maximum orbital velocity (Fig. 9h). At JB-4 site, the SSC shows high values more than 10 kg/m^3 in the wake of the storm (Fig. 9g). It is noted that the active migration of sand ripples could reduce the sensor elevation or even bury ADV probes, intermittently producing an extremely high SSC. At JB-4 site, the ADV backscatter signal was saturated over the detection limit at the night of 269 days due to severe sound attenuation (Fig. 9g) as shown in Ha et al. (2009). At JB-4 site, the location of sediment bottom corresponding to the maximum backscatter strength abruptly moved from 1.5 m to 1.4 m (Fig. 9h), reflecting some disturbance of TISDOS by strong storm-induced currents (oscillatory flows with speed of >1 m/s) and waves. Immediately after the storm passed, the backscatter strength at JB-4 site returned to the background concentration as a result of the rapid settling of suspended sands (Fig. 9h).

5. DISCUSSION AND CONCLUSIONS

The basically radial distribution of the coastal sand deposits from the stream mouths suggests that the coastal sands have originated predominantly from the Nagok, Bugu, and Jijeong

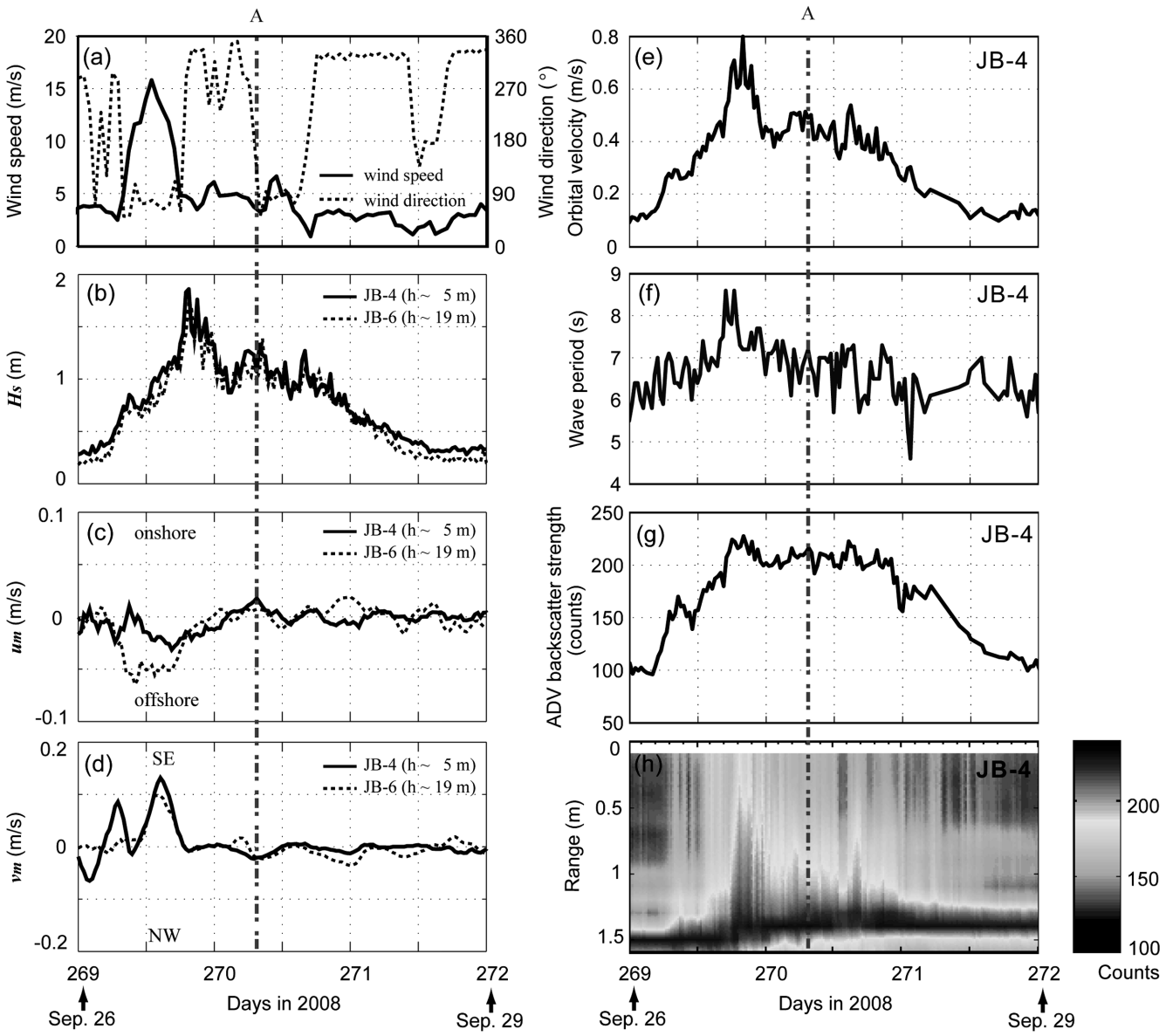

Fig. 9. TISDOS time series obtained during the passage of a storm. (a) wind speed and directions, (b) significant wave height, (c) cross-shore mean current velocity, (d) alongshore mean current velocity, (e) wave orbital velocity at JB-4 site, (f) wave period at JB-4 site, (g) suspended sediment concentrations (JB-4 site) from the OBS and ADV backscatter strength at 0.3 m above the seabed, and (h) ADCP backscatter strength within 1.5 m of the seabed at JB-4 site. Character 'A' denotes an 8.53-min burst interval (burst A, JB-4 site) for ensemble averaging analyses of wave cycles for major parameters.

streams. Even though these streams are associated with small drainage areas, their drainage areas in the nearby Taeback Mountains are very steep (2.23°–6.28°). Therefore, the flash floods during summer season (June-September) could episodically deliver a relatively large amount of terrigenous coarse sediments to the sea through these streams. This could be also supported by the mouth opening of Jijeong Stream for a short period of summer flash flooding (Fig. 2). The offshore pinch-out attribute of the sand deposit layer also attests to the terrigenous origin of the coastal sands. In addition, the SE-skewed elliptical isopach geometry of the coastal sands reflects that the run-off sediments have been most likely redistributed to the adjacent coastal and nearshore areas toward the southeast by alongshore coastal currents. During the transport, the wave reworking of the sands may be attested by their textural characteristics that show a coarsening trend in mean size from the stream mouth to the nearshore (Fig. 8).

The southeastward transport of the sands can be more quantitatively envisioned by the hydrodynamic measurements. The orbital velocities of storm waves in the nearshore (JB-4 site) would act as a prevalent hydrodynamic

forcing in sediment resuspension. Under the strongest storm winds, in addition, the cross-shore component of the mean currents directing the offshore (JB-4 site) implies that the resuspended sands then may be transported offshore. Earlier studies have reported that the dynamical interplay of strong wavy turbulences and mean flows in the near-bottom suspension contributes to significant sediment transports in the nearshore (Jaffe et al., 1985; Kraus and Larson, 1988; Russell, 1993). Therefore, the offshore-directed near-bottom flows most likely delivered large amounts of sands from the beach-nearshore area. The offshore sands (JB-6 site) transported from the beach-nearshore area could be further down-drifted (i.e., to the southeast) littorally by the SE-ward alongshore currents that were most likely substantial during the peak of storm. In this regard, the measurements, although of preliminary quality, clearly show that storm-derived mean currents could play a major role in distributing the coastal sands in the study area.

The hydrodynamic measurements additionally exhibit that the mean currents rapidly diminished after the peak of the storm (Figs. 9c and d). During the waning stage of storm with subdued wind speeds, the wave-induced turbulent mixing was still strong (or even grew) enough to maintain high SSC from vigorous resuspension of the bottom sands (Figs. 9g and h). These high-to-medium wave conditions would result in a steady onshore transport of the sands through flow-velocity skewness and asymmetry that are most visible in waves in wave shoaling zone just before on-set of wave breaking (Hanes and Huntley, 1986; Thornton et al., 1996; Russell and Huntley, 1999; Austin et al., 2009). Such shoaling processes of the wind waves can be seen in Figure 10 from an ensemble averaging analysis of waves in an 8.53-min burst interval recorded after the storm peak. In this analysis, the first one-tenth highest waves (i.e., corresponding to $H_{1/10}$) were separated and ensemble-averaged from individual waves in time-series trains since larger waves impact the sea bottom more strongly. The relatively steep and short crest of shoaling waves induces higher onshore velocity and acceleration, thereby causing larger onshore sediment transport compared to offshore sediment transports by the rather flat, broad trough (Fig. 10), as documented by Bailard (1981), Elgar et al. (2001), and Hsu and Hanes (2004). Therefore, the active erosion of nearshore sands by offshore mean currents during the short period of strongest storm winds may be roughly counteracted by onshore transport processes dominated by shoaling gravity-waves during the relatively longer period of the waning storm. In addition, the gravity waves higher than 0.5 m (corresponding to the critical wave orbital velocity, 0.2 m/s) could be frequently generated by offshore winds other than storms all year around (Fig. 3) and hence continually contribute to the onshore transport of the coastal sands.

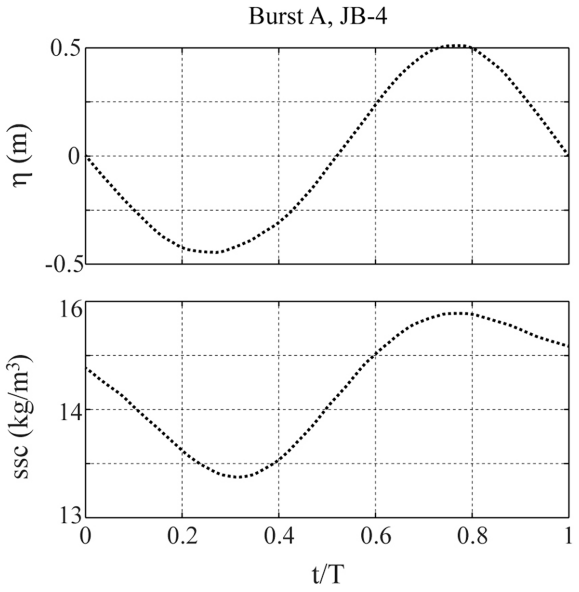

Fig. 10. Ensemble average of wave cycles in burst A (JB-4) for surface elevation (η), and suspended sediment concentration (SSC). For location of burst A in time series, see Figure 9.

ACKNOWLEDGMENTS: This work was supported by grants of the Korea Ocean Research and Development Institute (PE 98735) and the Center for Atmospheric Sciences & Earthquake Research (CATER 2012-8100). H.K. Ha was supported by the Korea Polar Research Institute's grant (PE10260). We thank Mrs. Su Hwan Lee, Jin Seok Ki and Jeong Min Lee for their technical assistance.

REFERENCES

Austin, M., Masselink, G., O'Hare, T., and Russell, P., 2009, Onshore sediment transport on a sandy beach under varied wave conditions: flow velocity skewness, wave asymmetry or bed ventilation? Marine Geology, 259, 86–101.

Bailard, J.A., 1981, An energetic total load sediment transport model for a plane sloping beach. Journal of Geophysical Research, 86, 10938–10954.

Damuth, J.E., 1980, Use of high-frequency (3.5–12 kHz) echograms in the study of near-bottom sedimentation processes in the deep-sea: a review. Marine Geology, 38, 51–75.

Dean, R.G. and Dalrymple, R.A., 1991, Water wave mechanics for engineers and scientists. Advanced Series on Ocean Engineering, Vol. 2. World Scientific, Singapore, 353 p.

Dyer, K.R., 1986, Coastal and Estuarine Sediment Dynamics. Wiley, New York, 342 p.

Elgar, S., Gallagher, E.L., and Guza, R.T., 2001, Nearshore sandbar migration. Journal of Geophysical Research, 106, 11623–11627.

Folk, R.L., 1954, The distinction between grain size and mineral composition in sedimentary rocks nomenclature. Journal of Geology, 62, 334-359.

Fredsøe, J. and Deigaard, R., 1992, Mechanics of Coastal Sediment Transport. World Scientific, London, 369 p.

Giosan, L., Donnelly, J.P., Vespremeanu, E., Bhattacharya, J.P., Olariu, C., and Buonaiuto, F., 2005, River delta morphodynamics: examples from the Danube delta. In: Giosan, L. and Bhattacharya, J.P. (eds.), River Deltas – Concepts, Models, and Examples. Society of Economic Paleontologists and Mineralogists, Special Publication, 83, 393–412.

Ha, H.K., Hsu, W.-Y., Maa, J.P.-Y., Shao, Y., and Holland, C.W., 2009, Using ADV backscatter strength for measuring suspended cohesive sediment concentrations. Continental Shelf Research, 29, 1310–1316.

Hanes, D.M. and Huntley, D.A., 1986, Continuous measurements of suspended sand concentration in a wave dominated nearshore environment. Continental Shelf Research, 6, 585−596.

Hsu, T.-J. and Hanes, D.M., 2004, Effects of wave shape on sheet flow sediment transport. Journal of Geophysical Research, 109, C05025.

Jaffe, B.E., Sternberg, R.W., and Sallenger, A.H., 1985, The role of suspended sediment in shore-normal beach profile changes. In: Proceeding of 19th Conference on Coastal Engineering. ASCE, Houston, p. 1983–1996.

KMA (Korea Meteorological Administration), 2009, Past weather database, *http://www.kma.go.kr*.

Komar, P.D., 1998, Beach Processes and Sedimentation. Prentice Hall, New Jersey, 544 p.

Kraus, N.C. and Larson, M., 1988, Beach profile change measured in the tank for large waves, 1956−1957 and 1962. Technical Report CERC-88-6, U.S. Army Corps of Engineers, Coastal Engineering Research Center, Vicksberg, 39 p.

Lee, S.W., 1999, A bibliography for neighboring waters of Korea. Jipmundang Co., Seoul, 344 p. (in Korean)

Longuet-Higgins, M.S., 1952, On the statistical distribution of the wave heights of sea waves. Journal of Marine Research, 11, 245–266.

McCall, R.T., Van Thiel de Vries, J.S.M., Plant, N.G., Van Dongeren, A.R., Roelvink, J.A., Thompson, D.M., and Reniers, A.J.H.M., 2010, Two-dimensional time dependent Hurricane overwash and erosional modeling at Santa Rosa Island. Coastal Engineering, 57, 668–683.

NIMR (National Institute of Meteorological Research), 2009, Wind waves 2008 database, *http://www.nimr.go.kr*.

Roelvink, D., Reniers, A., Van Dogeren, A., Van Thiel de Vries, J., McCall, R., and Lescinski, J., 2009, Modeling storm impacts on beaches, dunes and barrier islands. Coastal Engineering, 56, 1133–1152.

Russell, P.E., 1993, Mechanisms for beach erosion during storms. Continental Shelf Research, 13, 1243–1265.

Russell, P.E. and Huntley, D.A., 1999, A cross-shore transport "shape function" for high energy beaches. Journal of Coastal Research, 15, 198–205.

Sexton, W.J., Hayes, M.O., and Coloquhoun, D.J. 1992, Evolution of Auarwenary shoal complexes off the central South Carolina coast. In: Fletcher, C.H. and Wehmiller, J.F. (eds.), Quaternary Coasts of the United States: Marine and Lacustrine Systems. Society of Economic Paleontologists and Mineralogists, Special Publication, 48, 161–172.

Soomere, T., Kask, A., Kask, J., and Healy, T.R., 2008, Modeling of wave climate and sediment transport patterns at a tideless embayed beach, Pirita Beach, Estonia. Journal of Marine Systems, 74 (Supplement 1), S133–S146.

Snedden, J.W. and Nummedal, D., 1991, Origin and geometry of storm-deposited sand beds in modern sediments of the Texas continental shelf. In: Swift, D.J.P., Oertel, G.F., Tillman, R.W., and Thorne, J.A. (eds,), Shelf Sand and Sandstone Bodies: Geometry, Facies and Sequence Stratigraphy. International Association of Sedimentologists, Special Publication, 14, 283–308.

Soulsby, R., 1997, Dynamics of Marine Sands. Thomas Telford, London, 249 p.

Thornton, E.B., Humiston, R.T., and Birkermeir, W.A., 1996, Bar/trough generation on a natural beach. Journal of Geophysical Research, 101, 12097–12110.

Van Rijn, L.C., 1993, Principles of Sediment Transport in Rivers, Estuaries and Coastal Seas. Aqua Publications, Amsterdam, 715 p.

Manuscript received March 11, 2011
Manuscript accepted January 11, 2013